Deposition of Hydrogenated Amorphous Silicon Carbon Films Using Vacuum Ultraviolet Light

by

Tadashi FUJII*, Takashi FUYUKI* and Hiroyuki MATSUNAMI*

(Received June 24, 1992)

Abstract

Hydrogenated amorphous silicon carbon films are deposited using disilane and acetylene with vacuum ultraviolet light (147 nm) emitted from a microwave-excited Xe resonance lamp. The film shows a high photoconductivity of 1.2×10^{-5} S/cm at an optical bandgap of 2.0 eV which is one order larger than that of device-quality films deposited by a glow discharge (GD) method. Because of high photoconductivity in this film, over-hydrogenation of carbon atom is avoided, and tetrahedral bondings seem to form rigid random networks. For an application to the window layer of amorphous silicon-alloy solar cells, *p*-type doping properties are examined. In this case, a photoconductivity of 3.9×10^{-6} S/cm at an optical bandgap of 2.0 eV is obtained, which is comparable to that of device-quality films deposited by a GD method.

1. Introduction

Hydrogenated amorphous silicon carbon (a-SiC:H) films have been extensively studied for the application to the window layer of high-efficiency amorphous silicon-alloy solar cells. The films deposited by conventional glow discharge (GD) methods showed over-hydrogenation of carbon atoms. Rigid Si-C networks cannot be constructed owing to many CH_3 or CH_2 bonds.[1] Photoconductivity degrades with increasing carbon content in a-SiC:H films.

We have developed a novel CVD (chemical vapor deposition) method using VUV (vacuum ultraviolet) light (147 nm) emitted from a microwave-excited Xe resonance lamp. Photons with high energy can promote chemical reactions for the film deposition, which is expected to yield rigid amorphous networks with low hydrogen content. High-quality amorphous silicon films with low density of gap states[2] and stable photoconductivity under illumination[3] were realized.

In this study, the VUV photo-CVD method was applied to the deposition of a-SiC:H to obtain high photoconductivity with low hydrogen content. Source gases of disilane (Si_2H_6) and acetylene (C_2H_2) were directly decomposed by VUV light (147 nm). Material

* Department of Electrical Engineering II

properties were characterized concerned with film structure revealed by X-ray photoelectron spectroscopy (XPS) measurement and infrared (IR) spectroscopy measurement. Valency control was also investigated using diborane (B_2H_6).

2. Experiments

A schematic diagram of the apparatus is illustrated in Fig. 1. This apparatus consists of two parts; the left part is the light source and the right is the reaction chamber. Xe gas is discharged with a microwave of 2.45 GHz to emit a line at 147 nm. The emission intensity of Xe was promoted by He dilution. The optimized partial pressure of Xe and He were 5.0×10^{-2} Torr and 2.0 Torr, respectively. The emitted VUV light was led to the reaction chamber through the MgF_2 window. The back pressure of the reaction chamber was 1.0×10^{-4} Torr. The flow rates of Si_2H_6 and C_2H_2 were $5 \sim 10$ and $0.01 \sim 0.6$ sccm, respectively. During the film deposition, the window was blown by N_2 at a flow rate of 150 sccm to prevent the deposition of films on it. The total pressure of the reaction chamber during the deposition was 2.0 Torr. The substrate temperature was 250°C. The typical film thickness and deposition rate were 2000 Å and 3.5 Å/min, respectively, at a Si_2H_6 flow rate of 10 sccm. Quartz substrates were used for transmission, reflection, and conductivity measurements. Single crystalline silicon substrates were used for XPS and IR measurements.

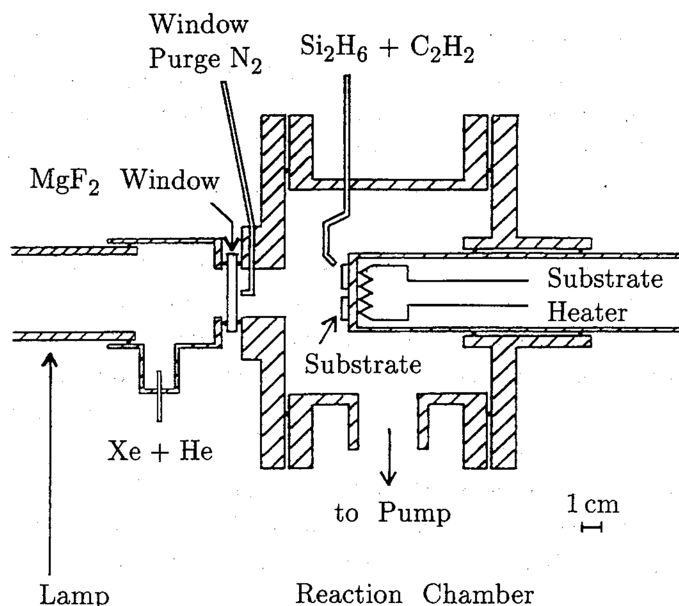

Fig. 1 Schematic diagram of VUV photo-CVD.

Photoconductivity was measured by planer structure with Al electrodes under the light of air mass 1 ($100\,mW/cm^2$) solar simulator.

3. Results and Discussions

3.1 Deposition Rate and Carbon Content

Figure 2 shows the deposition rate of a-SiC : H films as a function of the C_2H_2 fraction ($[C_2H_2]/([Si_2H_6]+[C_2H_2])$). The deposition rate gradually decreases with increasing C_2H_2 fraction. Figure 3 shows carbon content x as a function of the C_2H_2 fraction. The value of x was determined by XPS measurement using crystalline SiC as a reference. In the range of C_2H_2 fraction smaller than 2 %, x increases to 0.27 abruptly with increasing C_2H_2 fraction, but it increases gradually from 0.27 to 0.39 in the range of C_2H_2 fraction larger than 2 %. This result is almost the same as the case of a-SiC : H film deposition by low-pressure mercury lamp CVD using Si_2H_6 and C_2H_2.[4]

The reason for these results is thought to be as follows. Direct photolysis of Si_2H_6 using 147 nm VUV light has been reported in ref. 5.

$$(a)\quad Si_2H_6 + h\nu \rightarrow SiH_2 + SiH_3 + H \qquad (1)$$

$$(b)\quad Si_2H_6 + h\nu \rightarrow SiH_3SiH + 2H \qquad (2)$$

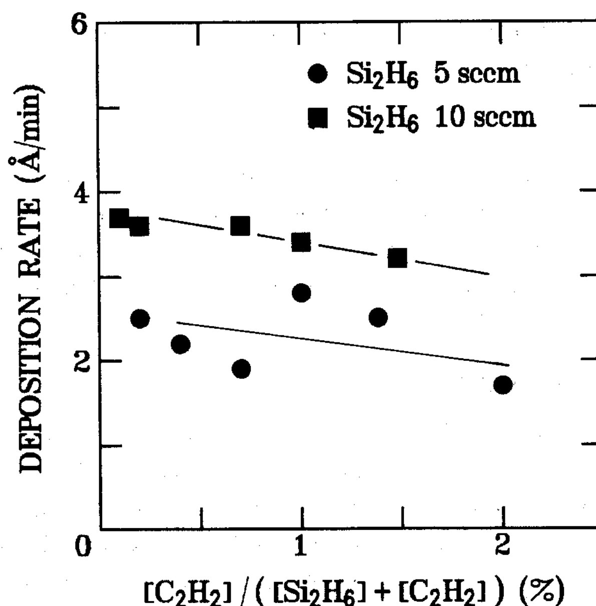

Fig. 2 Deposition rate as a functin of C_2H_2 fraction for Si_2H_6 flow rates of 5 sccm (■) and 10 sccm (●).

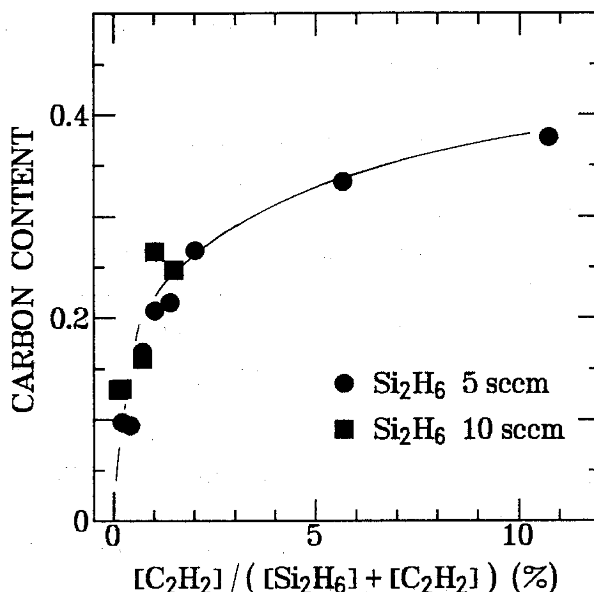

Fig. 3 Relative carbon content as a function of C_2H_2 fraction.

$$(c) \quad Si_2H_6 + h\nu \rightarrow Si_2H_5 + H \qquad (3)$$

The quantum yields of equations (1), (2), and (3) are 0.61, 0.18, and 0.21, respectively. The C_2H_2 molecules are directly decomposed by 147 nm VUV light as follows[6]:

$$C_2H_2 + h\nu \rightarrow C_2H + H \qquad (4)$$

The absorption cross section of Si_2H_6 and C_2H_2 at 147 nm are reported as $8.0 \times 10^{-17} cm^2$ [7] and $1.08 \times 10^{-17} cm^2$,[6] respectively. The absorption cross section of Si_2H_6 is 8 times larger than that of C_2H_2. Therefore, generation of atomic hydrogen is dominant in primary reactions by eqs. (1) ~ (3), and atomic hydrogens attack Si_2H_6 molecules and pull out Si_2H_5 radicals as follows[5]:

$$Si_2H_6 + H \rightarrow Si_2H_5 + H_2 \qquad (5)$$

It is supposed that at small C_2H_2 fraction a-Si : H is deposited from SiH_n radicals and a-SiC : H is deposited by the reaction of C_2H_2 and SiH_n radicals. However, at large C_2H_2 fraction, a-Si : H deposition decreases, and C_2H_2 molecules and Si_2H_5 radicals react with and make a precursor which directly changes to a-SiC : H on heated substrates. To explain this supposition, further experiments are needed, especially about the sticking coefficient of the above radicals.

3.2 Film Properties

3.2.1 Optical Bandgap and Conductivity

Absorption coefficient (α) and optical bandgap (E_{opt}) were measured by transmission and reflection measurements. From the equation of $(\alpha h\nu)^{\frac{1}{2}} = B^{\frac{1}{2}}(h\nu - E_{opt})$, E_{opt} was estimated and shown in Fig. 4 as a function of carbon content. The minimum value at $x = 0$ was for an a-Si : H film. The value of E_{opt} was found to increase linearly from 1.8 to 2.6 eV when x was varied from 0 to 0.34.

Figure 5 shows dark conductivity and photoconductivity of a-SiC : H films. Dark conductivity takes values of 10^{-10} S/cm regardless of the value of E_{opt}, and photoconductivity decreases from 1.2×10^{-5} to 2.9×10^{-8} S/cm with increasing E_{opt}. Photo sensitivity (the ratio of photoconductivity to dark conductivity) at an E_{opt} of 2.0 eV is 1.5×10^5 which is comparable to that of an a-Si : H film (E_{opt} : 1.8 eV). From this result, the a-SiC : H films deposited by VUV photo-CVD indicate high-quality. In Fig. 5, photoconductivity of a-SiC:H films deposited by a glow discharge (GD) method using SiH_4 and CH_4 is also shown.[8] The values of this experiment are about 10 times larger than that of GD films for all ranges of E_{opt} (2.0 ~ 2.2 eV).

3.2.2 Bond Configurations

To make clear why a-SiC : H films deposited by VUV photo-CVD indicate high

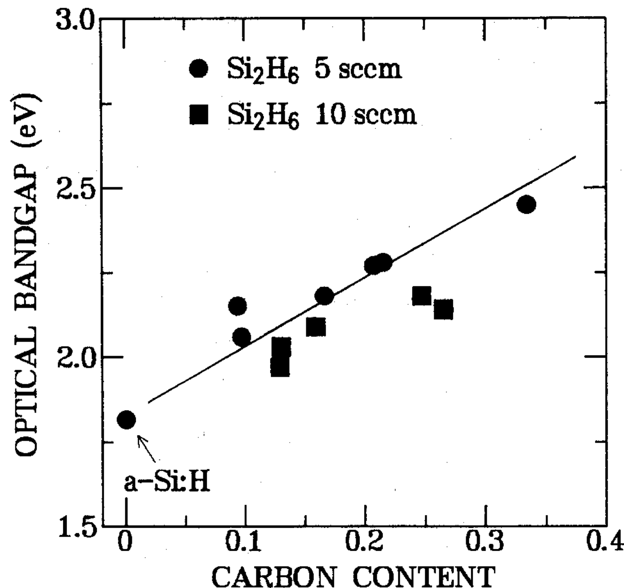

Fig. 4 Optical bandgap of a-SiC : H films as a function of carbon content.

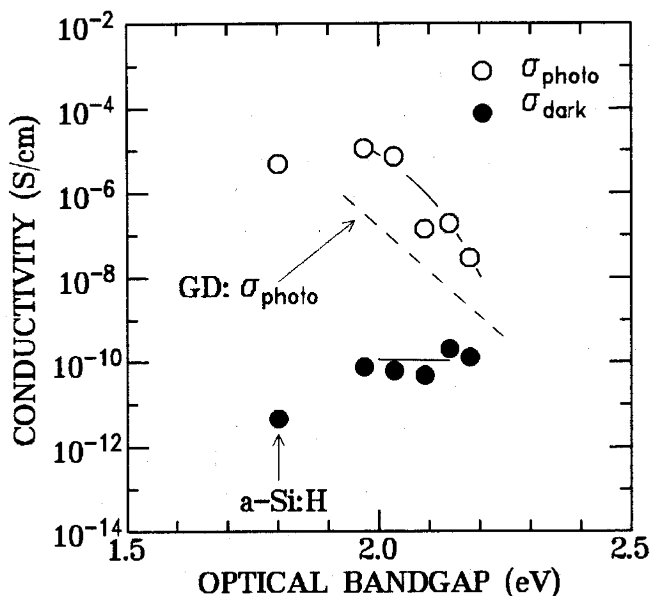

Fig. 5 Dark conductivity (●) and photoconductivity (○) of a-SiC : H films as a function of optical bandgap. Photoconductivity of GD films is indicated by dashed line.

photoconductivity, bond configurations of Si-Si, Si-C, and C-C in a-SiC : H films were investigated by analyzing XPS spectra of C(1s), Si(2s), and Si(2p). The reported binding energies of silicon and carbon in a-SiC : H are listed in Table 1.[9-11] AlK_α line (1486.6 eV) was used as the X-ray source and the resolution of the energy analyzer was 0.38 eV. To remove surface contamination and native oxide layers, films were sputtered for 3 minutes by Ar^+ before measurement. C(1s), Si(2s), and Si(2p) electron spectra around the binding energy of 285 eV, 152 eV, and 100 eV, respectively, were investigated. Each spectrum

Table. 1 Binding Energy of C- and Si-related bonds in a-SiC : H.[9-11]

	Binding Energy (eV)	Type
C(1s)	284.7 ~ 284.5	Graphite-like C
	284.3	$(CH_2)_n$
	283.6	Si-C in c-SiC
Si(2s)	155.6 ~ 151.8	Si-C in c-SiC
	154.0 ~ 151.6	Si-C in a-SiC : H
	150.6 ~ 150.4	Si-Si in c-Si
Si(2p)	103.0	Si in $Si\text{-}CH_3$ or O
	100.2	Si-C in c-SiC
	99.3	Si-Si in a-Si : H

c : crystalline a : amorphous

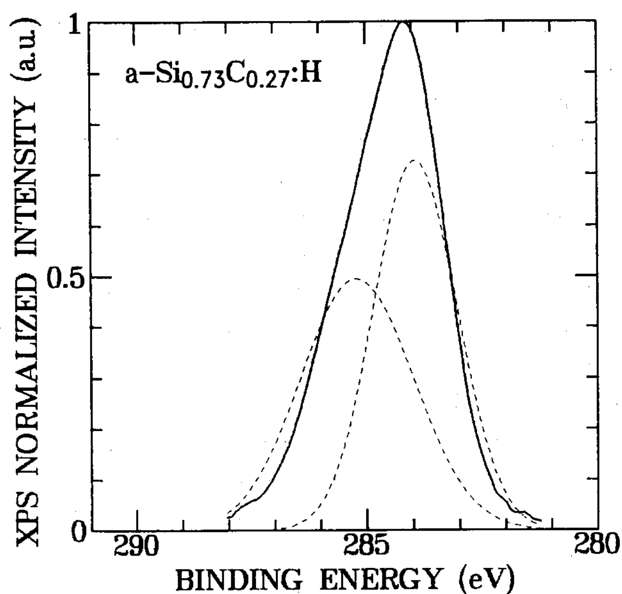

Fig. 6 Example of peak deconvolution for C(1s) XPS spectrum.

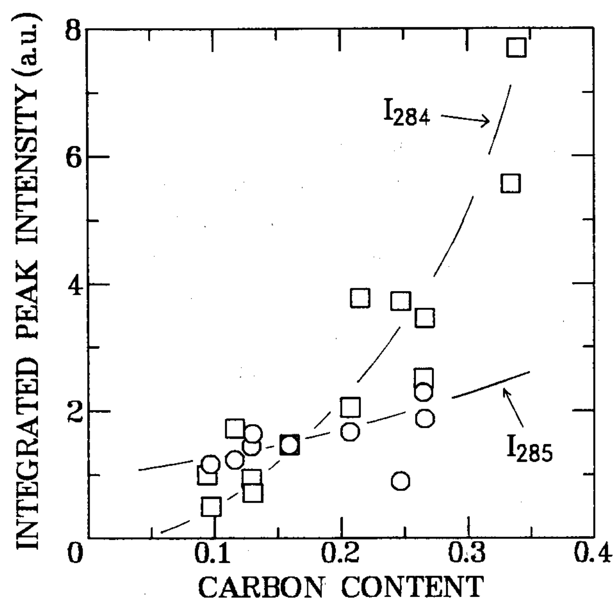

Fig. 7 Integrated intensity of 284 eV peak (□) and 285 eV peak (○).

consisted of some components originating from different bond configurations. The spectra were deconvoluted by assuming that every peak has Gaussian distribution.

C(1s) electron spectra have two peaks near 285 eV and near 284 eV. Original and deconvoluted spectra are shown in Fig. 6. The peak around 285 eV is due to graphite-like carbon,[9] and the peak near 284 eV is due to $(CH_2)_n$ chains or Si-C bonds.[10] Figure 7 shows integrated peak intensities of near 285 eV (I_{285}) and near 284 eV (I_{284}). I_{285} increases gradually with increasing carbon content, however, I_{284} increases abruptly with carbon content. From IR measurement, C-H bond concentration decreased drastically with increasing carbon content, so we suggest that the 284 eV peak does not originate from $(CH_2)_n$ chains, but from Si-C bonds. This means that tetrahedral bondings, which dominantly consisted of Si-C bond, formed rigid random structures.

Hydrogen concentration and bonding state in an a-SiC:H film affect the optical and electrical properties of the film. In this experiment, IR absorption was measured using Fourier transform infrared spectroscopy. Si-H bond concentration [Si-H] and C-H bond concentration [C-H] were calculated from the integrated absorption strength for Si-H_n stretching modes around 2100 cm^{-1} and C-H_n stretching modes around 2950 cm^{-1}, respectively, according to the following equations:

$$[\text{Si-H}] = A_{\text{Si-H}} \int \frac{\alpha}{\omega} d\omega, \tag{6}$$

$$[\text{C-H}] = A_{\text{C-H}} \int \frac{\alpha}{\omega} d\omega, \tag{7}$$

where the proportionality constant $A_{\text{Si-H}}$ of 1.4×10^{20} cm^{-2}[12] and $A_{\text{C-H}}$ of 1.0×10^{21} cm^{-2},[13] were used in the calculation.

The average number of hydrogen atoms attached to a Si atom ([Si-H]/[Si]), that to a C atom ([C-H]/[C]), and total hydrogen content (C_H) in a-SiC:H films are shown in Figs. 8, 9, and 10, respectively, as a function of carbon content. In these figures, typical values reported on GD films[13] are also shown by dashed lines. [Si-H]/[Si] increased monotonously from 0.05 to 0.39 with increasing carbon content. [C-H]/[C] decreased monotonously from 1.46 to 0.25 with increasing carbon content. C_H was calculated from the next equation.

$$C_H = (1-x) \times \frac{[\text{Si-H}]}{[\text{Si}]} + x \times \frac{[\text{C-H}]}{[\text{C}]}. \tag{8}$$

In equation (8), x means carbon content of the film. The value of C_H increases in the range of carbon content smaller than 0.15, however, it decreases gradually in the range of carbon content above 0.15 for the reason that [C-H]/[C] decreases with increasing in carbon content. Conversely, the value of C_H in a-SiC:H films deposited by a GD method

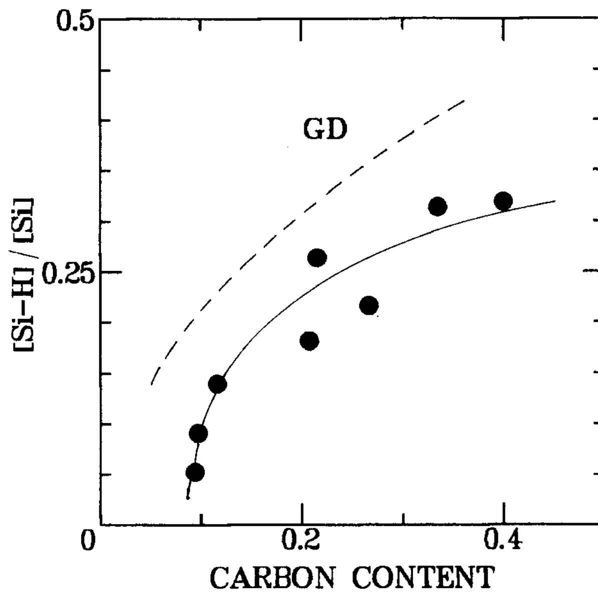

Fig. 8 Average number of hydrogen atoms attached to a Si atom as a function of carbon content. The value of GD films is indicated by dashed line.

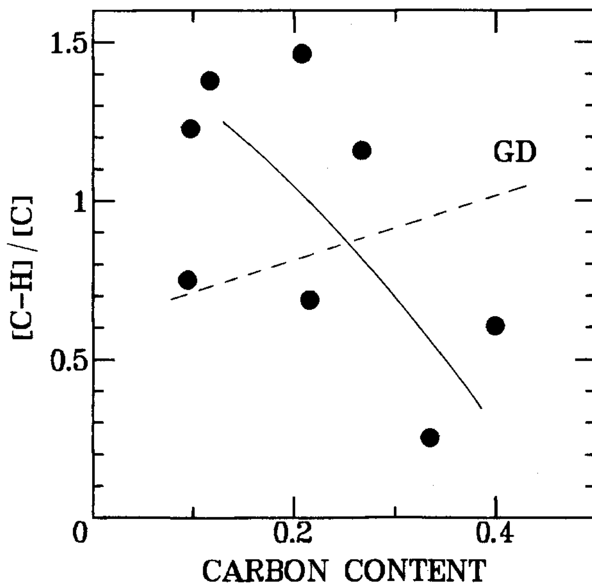

Fig. 9 Average number of hydrogen atoms attached to a C atom as a function of carbon content. The value of GD films is indicated by dashed line.

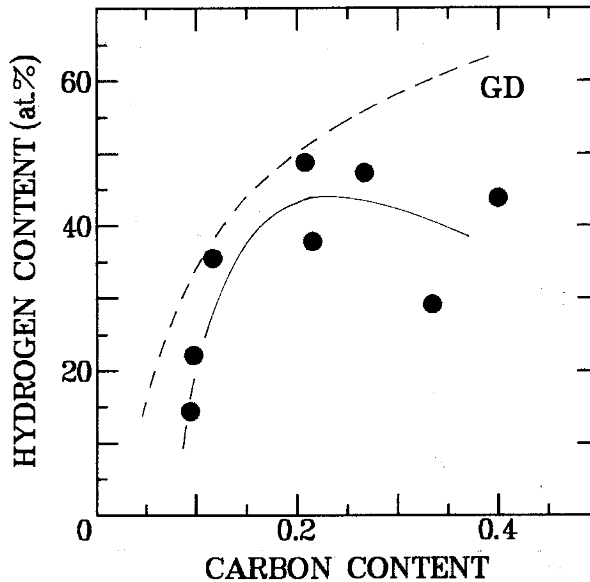

Fig. 10 Hydrogen Content as a function of carbon content. The value of GD films is indicated by dashed line.

shows monotonous increase as a function of carbon content for the reason that both [C-H]/[C] and [Si-H]/[Si] increase monotonously. From this result, a-SiC:H films deposited in this study have small C_H especially in large carbon content compared to GD films, which may lead to rigid random networks.

3.3 Properties of Boron-Doped Films

For an application to a-Si solar cells, *p*-type doping was studied using B_2H_6. Figure 11 shows the optical bandgap of a-SiC:H films as a function of B_2H_6 fraction ($[B_2H_6]/([Si_2H_6] + [C_2H_2] + [B_2H_6])$). The value of E_{opt} must be larger than that of undoped a-Si:H to transmit the light without absorption. In this experiment, the C_2H_2 fraction was fixed to obtain $E_{opt} = 2.0\,eV$ (carbon content: 0.13). The value of E_{opt} was almost constant in the range of B_2H_6 fraction smaller than 1.0×10^{-2}, however, bandgap narrowing occurred in the large B_2H_6 fraction. From this result, the maximum B_2H_6 fraction was taken as 1.0×10^{-2}.

High photoconductivity is also needed for the window layer to reduce the series resistance of the solar cell. Figure 12 shows the relation of E_{opt} and photoconductivity in boron-doped a-SiC:H films. Photoconductivity decreases with increasing E_{opt} gradually in the order of $10^{-6}\,S/cm$ until $E_{opt} = 2.0\,eV$, but abruptly decreases beyond $E_{opt} = 2.0\,eV$. In Fig. 12, the photoconductivity of a-SiC:H films deposited by GD methods is shown at $E_{opt} = 2.0\,eV$.[14] The result in this experiment is comparable to GD films at $E_{opt} = 2.0\,eV$.

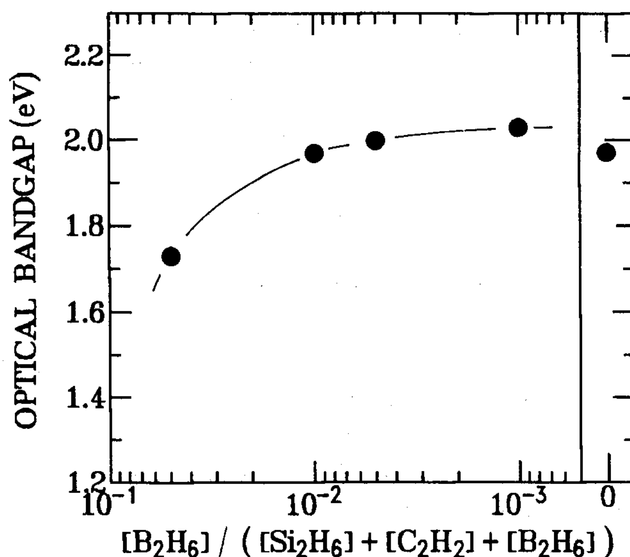

Fig. 11 Optical bandgap as a function of B_2H_6 doping rate.

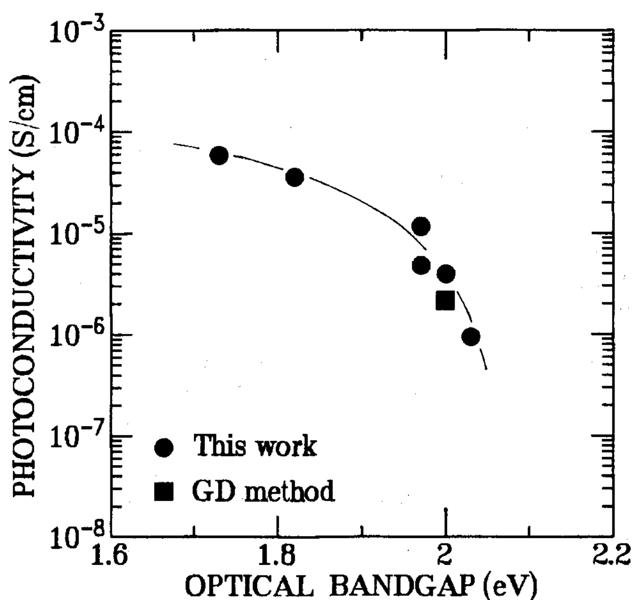

Fig. 12 Relation of optical bandgap and photoconductivity in boron doped a-SiC : H films.

Generally, B_2H_6 is decomposed insufficiently not only in a GD method but also in a photo-CVD process. B-B and B-H bonds are thought to remain easily in a-SiC : H films, resulting in high defect densities and low photoconductivity. Recently new type doping

gases, such as trimethylboron ($B(CH_3)_3$) and triethylboron ($B(C_2H_5)_3$), have been investigated for the reason that these gases are easily decomposed by photon energy, and high photoconductivity is obtained by low-pressure mercury lamp CVD.[15] To get higher photoconductivity, it is important to find out such a doping gas for our process.

4. Conclusion

a-SiC:H films are deposited by direct photo-CVD using vacuum ultraviolet light (147 nm). The film indicates a high photoconductivity of 1.2×10^{-5} S/cm at an optical bandgap of 2.0 eV, which is one order larger than that of device-quality films deposited by GD methods. For the reason of high photoconductivity (1.2×10^{-5} S/cm) in this film, over-hydrogenation of carbon atom is avoided, and tetrahedral bondings seem to form rigid random networks revealed from XPS and IR measurements. For application to the window layer of amorphous silicon-alloy solar cells, boron doped films were examined. In this case, this film shows a photoconductivity of 3.9×10^{-6} S/cm at an optical bandgap of 2.0 eV which is comparable to films deposited by GD methods.

References

1) A. Morimoto, T. Niura, M. Kumeda and T. Shimizu; J. Appl. Phys.; **53**, 7299, (1982).
2) T. Shirafuji, M. Yoshimoto, T. Fuyuki and H. Matsunami; Jpn. J. Appl. Phys.; **30**, L538, (1991).
3) T. Fuyuki, K. Y. Du, S. Okamoto, S. Yasuda, T. Kimoto, M. Yoshimoto and H. Matsunami; J. Appl. Phys.; **64**, 2380, (1988).
4) Y. Tarui, K. Kamisako, H. Yamazaki, K. Ishihara and T. Satoh; ENERGY CONVERSION AND UTILIZATION WITH HIGH EFICIENCY Subarea C, Science and Technology for Energy Conversion; P. 119 Dec. (1990).
5) G. G. A. Perkins and F. W. Lampe; J. Am. Chem. Soc.; **102**, 3764, (1980).
6) H. Okabe; J. Chem. Phys.; **75**, 2772, (1981).
7) U. Itoh, Y. Toyoshima, H. Onuki, N. Washida and T. Ibuki; J. Chem. Phys.; **85**, 4867, (1986).
8) S. Tsuda, H. Tarui, T. Matsuyama, T. Takahashi, S. Nakayama, Y. Hishikawa, N. Nakamura, T. Fukatsu, M. Ohnishi, S. Nakano and Y. Kuwano: Jpn. J. Appl. Phys.; **26**, 28, (1987).
9) T. Shimizu; J. Non-Cryst.; **59/60**, 117, (1983).
10) S. Suzuki, S. Meikle, Y. Fukuda and Y. Hatanaka; Jpn. J. Appl. Phys.; **29**, L663, (1990).
11) J. P. Gerault, R. Morancho, G. Constant, P. Mazerolles, J. J. Ehrhardt and M. Alnot; Thin Solid Films; **101**, 83, (1983).
12) H. Weider, M. Cardona and C. R. Gaurnieri; Phys. Stat. Sol. (b); **92**, 99, (1979).
13) F. Fujimoto, A. Ootuka, K. Komaki, Y. Iwata, I. Yamane, H. Yamashita, Y. Hashimoto, Y. Tawada, K. Nishimura, H. Okamoto and Y. Hamakawa; Jpn. J. Appl. Phys.; **23**, L810, (1984).
14) H. Tarui, T. Matsuyama, S. Okamoto, H. Dohjoh, Y. Hishikawa, N. Nakamura, S. Tsuda, S. Nakano, M. Ohnishi and Y. Kuwano; Jpn. J. Appl. Phys.; **28**, 2436, (1989).
15) K. Tabuchi, A. Yamada, M. Konagai and K. Takahashi; Jpn. J. Apl. Phys.; **11A**, 2742, (1991).